

# New insights on the PBTI phenomena in SiON pMOSFETs

K. Rott<sup>a,\*</sup>, H. Reisinger<sup>a</sup>, S. Aresu<sup>a</sup>, C. Schlünder<sup>a</sup>, K. Kölpin<sup>a</sup>, W. Gustin<sup>a</sup>, T. Grasser<sup>b</sup>

<sup>a</sup>Infineon Technologies AG, D-85579 Munich, Germany

<sup>b</sup>Institute for Microelectronics, TU Wien, A-1040 Vienna, Austria

## ARTICLE INFO

### Article history:

Received 5 June 2012

Received in revised form 12 June 2012

Accepted 13 June 2012

Available online 6 July 2012

## ABSTRACT

The physical origin of both Negative- and Positive Bias Temperature Instability (N-/PBTI) is still unclear and under debate. We analyzed the rarely studied recovery behavior after PBTI stress in pMOSFETs and compared it with NBTI data obtained from the same technology. While recovery after short stress times is consistent with the previously reported emission of trapped holes, for stress times larger than 10 ks we observe an unusual recovery behavior not reported before. There, the device degradation appears to continue during recovery up to approximately 30 s. Only after that time “normal” recovery behavior dominates. We thoroughly analyze this new observation as this may have significant consequences regarding our understanding of both PBTI and NBTI.

© 2012 Elsevier Ltd. All rights reserved.

## 1. Introduction

Hundreds of studies have been performed on NBTI phenomena in pMOSFETs [1,2], but only very few focused on PBTI [2,3]. This is possibly based on the assumption that PBTI in SiON pMOSFETs is less important than NBTI as the PBTI stress condition does not regularly occur in pMOSFETs devices in logic circuits. However, it has recently been pointed out that PBTI can be a regular stress condition for pMOSFETs in basic analog building blocks, especially during power-down-mode at elevated temperatures [5]. In [3,4] the PBTI effect has been identified as trapping of positive charge in the oxide, similarly to the NBTI mechanism. However, while during NBTI this positive charge is injected from the p-channel into oxide-traps near the substrate-oxide interface, during PBTI the injection occurs from the p-poly gate into oxide-traps near the interface between gate-electrode and gate-oxide. Thus both PBTI and NBTI in pMOSFETs cause a negative  $\Delta V_T$  [6]. In this work it is shown that the PBTI effect is actually more complicated to describe and model than believed previously. Compared to NBTI, recovery is no longer monotonous after a certain stress time. Quite to the contrary, the devices initially appear to keep degrading at the recovery voltage and “normal” recovery only sets in after longer recovery times. This phenomenon makes lifetime projections far less reliable than those made for NBTI. On the other hand, this may provide us with a unique opportunity for further insights into the physical processes involved in BTI.

## 2. Samples & measuring technique

The samples analyzed in this study are from production-quality 90 nm-technology with plasma nitrided oxides. The oxide thick-

nesses are 1.8 nm, 5.8 nm and 25 nm. Only the 5.8 nm data is shown here. While the other oxides show similar behavior as the 5.8 nm oxide, the normalized magnitude of degradation ( $\Delta V_T/t_{ox}$ ) is different due to the thickness-dependent concentration of nitrogen at the oxide-gate interfaces. Degradation and recovery of threshold voltage after stress have been measured using our ultra-fast (1  $\mu$ s) and high resolution (<1 mV) MSM technique [7].

## 3. Comparison of NBTI and PBTI

Fig. 1 shows the results of the recovery behavior of an accelerated stress test performed at a field of  $\approx 7$  MV/cm for NBTI and PBTI with stress times up to 10 ks. At a first glance PBTI behaves just like NBTI: the PBTI effect is smaller than NBTI by a factor of 3, as previously found [3–5]. This factor 3 can be roughly explained by a geometry effect,

$$\Delta V_T = \frac{Q_{trap}}{C_{ox}} \times \frac{x}{t_{ox}}, \quad (1)$$

where  $\Delta V_T$  is the threshold voltage shift,  $Q_{trap}$  the trapped charge sheet,  $C_{ox}$  the oxide capacitance,  $t_{ox}$  the oxide thickness and  $x$  the averaged position of the trapped charge. The “PBTI-defects” at the oxide-gate interface are further away from the inversion layer than the “NBTI-defects” and thus the electro-statically induced charge in the channel is smaller than from the “NBTI-defects” (see Figs. 2 and 1). As shown in Fig. 1, the amount of recovery after a stress time  $t_s = 10$  ks and between recovery times  $t_r = 1 \mu$ s and 10 s, is roughly 30% of the initial  $\Delta V_T$ . Thus, at a first glance the recovery behavior appears similar for NBTI and PBTI. One obtains quite a different picture when looking lower stress voltages as shown in Fig. 3. Compared to Fig. 1 the stress field has been reduced to a value of 4.5 MV/cm (only 10% above use condition) and the thermally acti-

\* Corresponding author. Tel.: +49 89 234 22237; fax: +49 89 234 9555496.

E-mail address: [karina.rott@infineon.com](mailto:karina.rott@infineon.com) (K. Rott).

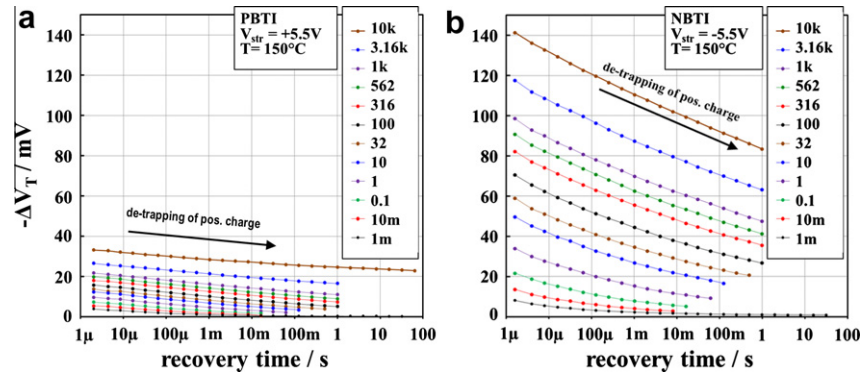


**Fig. 1.** Comparison of recovery traces for PBTI and NBTI for the same type of pMOSFETs with  $t_{ox} = 5.8$  nm. The stress-time corresponding to each trace (1 ms ... 10 ks) is given in the legend (in s).

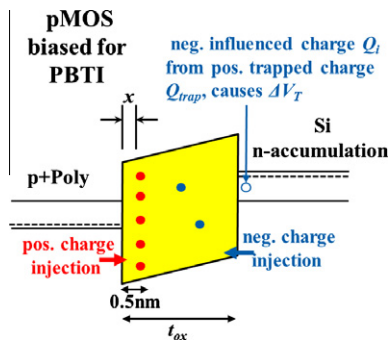


**Fig. 2.** Band diagram of oxide with interfaces, defects (schematic) and the processes during PBTI.

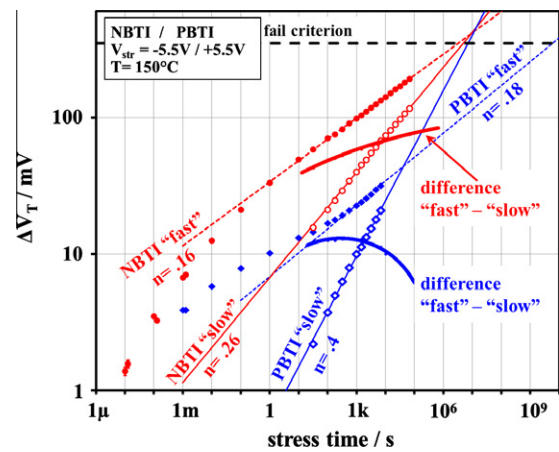


**Fig. 4.**  $\Delta V_T$  vs. stress time for NBTI and PBTI for a fast (1  $\mu$ s) and a slow (1 s) measuring delay. “fast” and “slow”  $\Delta V_T$  are not from different FETs but from the same recovery traces. Note the vast differences in the power-law exponents  $n$  and the seemingly perfect fit to straight lines.

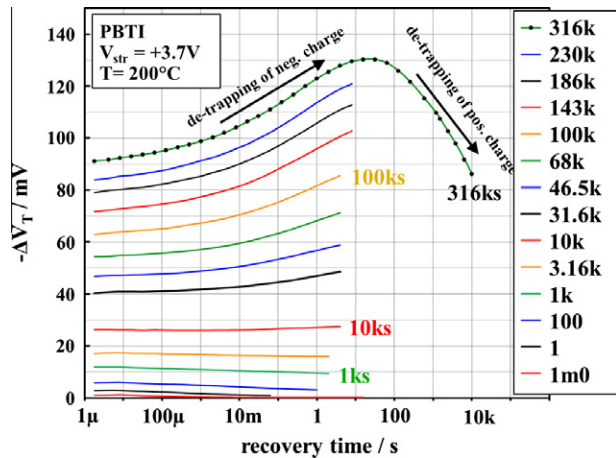


**Fig. 3.** Recovery traces like in Fig. 1 but for a low stress-voltage only 10% above the operating voltage and long stress times, accelerated by high  $T$ . An additional degradation mechanism is revealed by the anomalous “reverse” recovery behavior for stress time > 10 ks.

vated charge capture processes [8] have been accelerated by roughly a factor 10 (taken from Fig. 8) by increasing the temperature. While for stress times < 1 ks normal recovery behavior occurs, for longer stress times the sign of recovery reverses, i.e.  $\Delta V_T$  increases with recovery time. For the final recovery trace (after stress 316 ks) at  $T = 200$  °C, this reverse recovery continues until recovery time  $t_r \sim 30$  s and afterwards is followed by normal recovery for  $t_r > 30$  s.

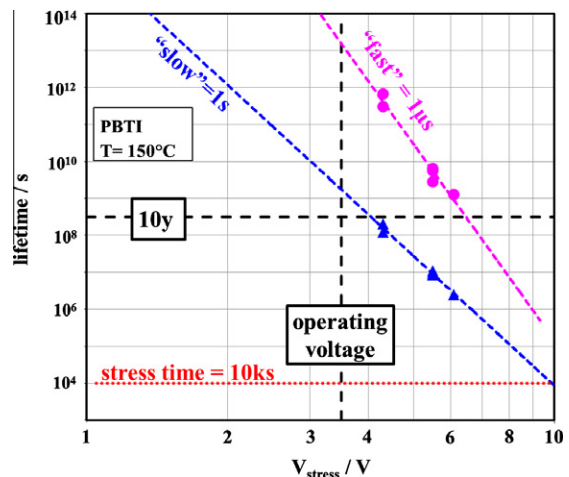


**Fig. 5.** Lifetime projection from the same set of data w.r.t. short stress times (10 ks) for a “slow” and a “fast” measuring delay for three stress voltages.

#### 4. Consequences for lifetime assessments

Examples for measured and extrapolated  $\Delta V_T$ 's vs. time and for a lifetime projection are given in Figs. 4 and 5. The lifetime projection is based on 10 ks stress-times as for a typical qualification.

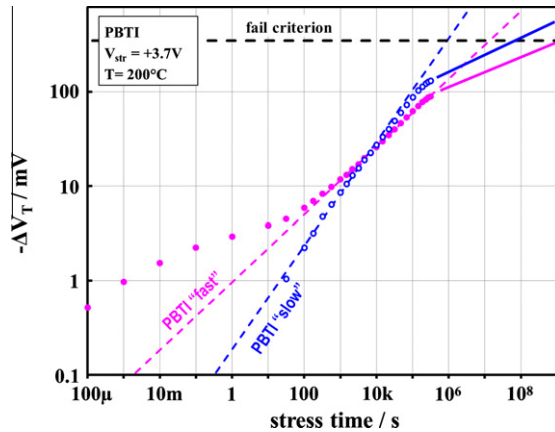


**Fig. 6.**  $\Delta V_T$  vs. stress time like in Fig. 4 but from low field and long stress. Note the dramatic lifetime-differences between extrapolation from  $t_{str} = 10$  ks (dashed lines) and  $t_{str} = 300$  ks and between “fast” and “slow”. No more straight lines.

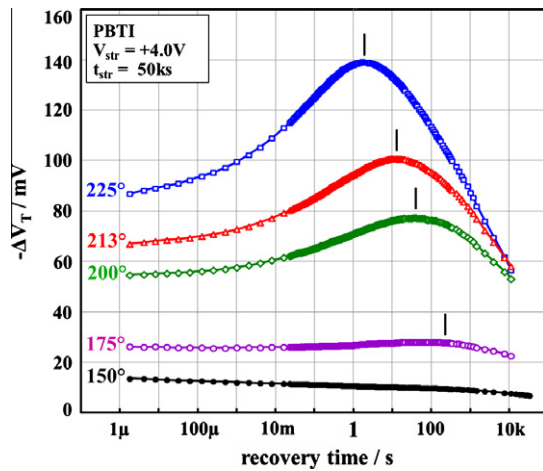


**Fig. 7.** “Anomalous” recovery traces like in Fig. 3 for different temperatures. The position of the peak-time is marked.

Data for a short and a long measuring delay are compared. It has been long known that the measuring delay has a significant influence on the power-law exponent for NBTI [9]. As seen in Figs. 4 and 5 this influence is dramatically larger for PBTI compared to NBTI. Fig. 6 shows that the reverse recovery even leads to a crossover of “slow” and “fast”  $\Delta V_T$  vs. stress-time.  $\Delta V_T$  for long stress times ( $>100$  ks) strongly deviates from the initial (after 10 ks) power-law thus leading to a change in extrapolated lifetimes as a function of the stress time by orders of magnitudes. For NBTI it is mostly accepted that correct lifetime assessments require a short measuring delay. Given our results, however, it is by no means clear how correct data for a PBTI assessment are to be generated, i.e. if a short or rather a long measuring delay leads to correct assessment. At present the best way appears to be to employ very long stress tests and a moderate voltage acceleration like shown in Fig. 6. As this is clearly unsatisfactory from a qualification perspective, a better understanding of the phenomenon is mandatory.

## 5. Discussion of physical processes

The most obvious explanation – indicated in Fig. 2 – for the observed reverse recovery is to assume negatively charged traps as reported in [10]. In addition to the positive charge injected into the “positive traps” at the poly-oxide interface, it seems that there

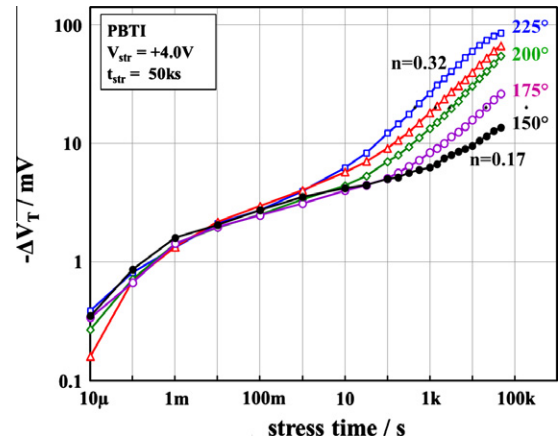


**Fig. 8.**  $\Delta V_T$  vs. stress time – corresponding to recovery traces in Fig. 7 – for different temperatures. Power law exponent values for the temperature 225 °C and 150 °C, respectively.

are traps (somewhere in the oxide) which can become negatively charged. Both polarities of traps discharge after the field is switched from (+7 MV/cm) to a value close to zero (recovery at  $V_T$ ). Negatively charged defects apparently have a shorter emission time than the positive ones (cmp. Figs. 7 and 10).

In total, “normal” PBTI always dominates, but the ratio between negative and positive charge  $Q^-/Q^+$  increases with decreasing field as well as for long stress times. The same “reverse” recovery behavior can be observed in narrow devices with the  $W/L$  (width to length) ratio of 0.12/0.08  $\mu\text{m}$ , as shown in Fig. 11. Measurements on such small devices show the charging of single defects as discrete steps in  $V_T$ . Unfortunately, statistical analysis is very challenging because of the long stress and recovery times [11]. However, it is clear from the discrete steps up in the recovery traces that a stochastic process like capture of positive or emission of negative charges occurs. Unfortunately, an unambiguous separation of positive and negative charge trapping is difficult due to compensation. If the amount of positive and negative charges is equal, there is no effect. In an attempt to separate the two contributions, we look at those recovery traces showing a peak (like the top trace in Fig. 3). Starting from a stress condition resulting in the occurrence of a peak in the recovery trace, the parameters temper-

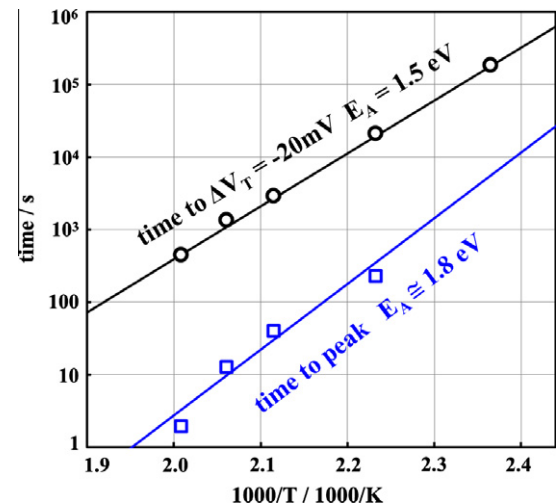


**Fig. 9.** Arrhenius plot from the peak-times in Fig. 7 and the time to reach  $\Delta V_T = 20$  mV in Fig. 8.

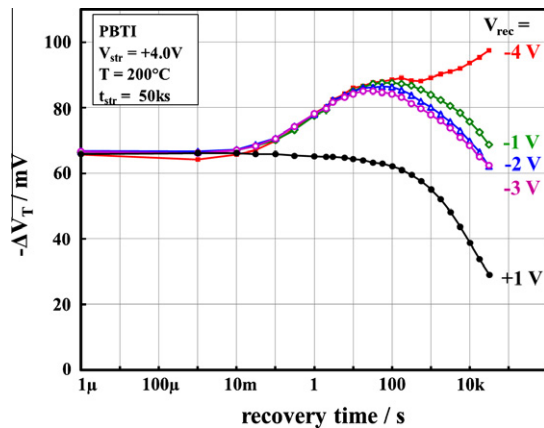


Fig. 10. Recovery traces like in Fig. 7 at 200 °C but done at recovery voltages below or above threshold to speed up or slow down recovery.

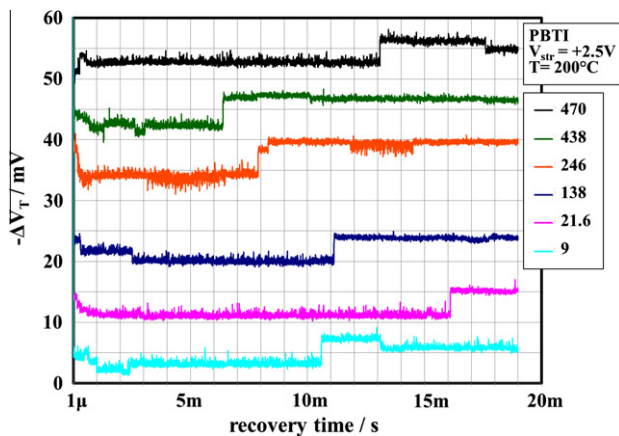


Fig. 11. An example of “reverse” recovery traces on a single narrow pMOSFET ( $W = 0.12 \mu\text{m}$ ,  $L = 0.08 \mu\text{m}$ ). Discrete steps up show the capture of positive charge into defects during the recovery. The stress-time corresponding to each trace is given in the legend (in s).

ature (shown in Figs. 7 and 8) and recovery voltage (shown in Fig. 10) have been varied. The thermal activation is analyzed in the Arrhenius plot Fig. 9. Effective activation energies are higher than those typically observed for NBTI ( $E_A \cong 0.6 \text{ eV}$ ) [11], but this may be an experimental artifact due to the distortion of the curves by mixed trapping of both polarities. The shift of the recovery peak as a function of  $T$  in Figs. 7 and 9 indicates that both hole and electron de-trapping speed up when  $T$  is increased.

The effect of recovery voltage after PBTI on the recovery of  $\Delta V_T$  is shown in Fig. 10. When starting with a recovery voltage near  $V_T = -400 \text{ mV}$  and going to more negative recovery voltages the recovery – mainly where hole de-trapping dominates – is accelerated, as expected. When the “recovery” voltage is below  $-4.0 \text{ V}$  the “normal” NBTI degradation “takes over” and  $|\Delta V_T|$  increases (i.e. accumulates degradation) rather than recovers.

On the other hand, it appears that the assumed electron de-trapping is – contrary to expectation for switching traps [11] – independent of the recovery voltage, and hole de-trapping vanishes for

positive recovery voltages. This behavior, together with the fact, that the “fast”  $\Delta V_T$  vs. stress time (see Figs. 4 and 6) is just the standard power-law with  $n = 0.18$ , rather support another hypothesis: PBTI stress creates a neutral precursor invisible during degradation, which becomes charged positively during recovery and “anneals” after a typ. time of  $<100 \text{ s}$  (see Fig. 7) as suggested in [12]. Such a model without e-trapping during degradation would explain why there is no deviation from a perfect power-law for the “fast” measurements (see Fig. 6.).

## 6. Conclusions

During the PBTI degradation of SiON pMOSFETs we have observed an additional component leading to the occurrence of an unexpected reverse recovery. This additional component severely distorts all extrapolations ( $\Delta V_T$  vs. time,  $\Delta V_T$  vs. operating voltage) usually done for lifetime projections. Thus, the analysis of PBTI data is more complex than of NBTI data. As such, a conclusive identification of the physical processes involved in PBTI phenomena in pMOS is more complicated than assumed but necessary for reliable life-time estimation.

## Acknowledgment

The research leading to these results has received funding from the European Community's FP7 Project No. 261868 (MORDRED).

## References

- [1] Stathis JH, Zafar S. The negative bias temperature instability in MOS devices: a review. *Microelectron Reliab* 2006;46(2–4):270.
- [2] Grasser T, Kaczer B, Gös W, Reisinger H, Aichinger T, Hehenberger Ph, et al. The paradigm shift in understanding the bias temperature instability: from reaction-diffusion to switching oxide traps. *IEEE Trans Electron Dev* 2011;58(11):3652.
- [3] Hehenberger Ph, Reisinger H, Grasser T. Recovery of negative and positive bias temperature stress in pMOSFETs. In: Final report of IEEE international integrated reliability workshop; 2010. p. 8.
- [4] Toledano-Luque M, Kaczer B, Roussel PhJ, Franco J, Ragnarsson LÅ, Grasser T, et al. Depth localization of positive charge trapped in silicon oxynitride field effect transistors after positive and negative gate bias temperature stress. *Appl Phys Lett* 2011;98:183506.
- [5] Schluender C, Reisinger H, Aresu S, Gustin W. On the PBTI degradation of pMOSFETs and impact on IC lifetime. In: Integrated reliability workshop final report; 2011. p. 7.
- [6] Grasser T, Kaczer B, Hehenberger Ph, Gös W, Connor R, Reisinger H, et al. Simultaneous extraction of recoverable and permanent components contributing to bias-temperature instability. In: International electron devices meeting; 2007. p. 801.
- [7] Reisinger H, Blank O, Heinrigs W, Gustin W, Schluender C. A comparison of very fast to very slow components in degradation and recovery due to NBTI and bulk hole trapping to existing physical models. *IEEE Trans Dev Mater Reliab* 2007;7(1):119.
- [8] Grasser T. Stochastic charge trapping in oxides: from random telegraph noise to bias temperature instabilities. *Microelectron Reliab* 2012;52(1):39.
- [9] Rangan S, Miele N, Yeh ECC. Universal recovery behavior of negative bias temperature instability [pMOSFETs]. In: Technical digest IEEE international electron device meeting; 2003. p. 1431.
- [10] Campbell JP, Cheung KP, Suehle JS, Oates A. Electron trapping: an unexpected mechanism of NBTI and its implications. In: Symposium on VLSI technology digest of technical papers; 2008. p. 76.
- [11] Grasser T, Reisinger H, Wagner P-J, Kaczer B. Time-dependent defect spectroscopy for characterization of border traps in metal-oxide-semiconductor transistor. *Phys Rev B* 2010;82(24):5318. 1.
- [12] Grasser T, Aichinger T, Pobegen G, Reisinger H, Wagner P-J, Franco J, et al. The ‘permanent’ component of NBTI: composition and annealing. In: Conference proceedings of international reliability physics symposium; 2011. p. 605.